Dynamical properties of the hexagonal close-packed metals Sc, Y, and Ru

2002 J. Phys.: Condens. Matter 14 4669

(http://iopscience.iop.org/0953-8984/14/18/304)

INSTITUTE OF PHYSICS PUBLISHING JOURNAL OF PHYSICS: CONDENSED MATTER

J. Phys.: Condens. Matter **14** (2002) 4669–4677 PII: S0953-8984(02)34554-5

Dynamical properties of the hexagonal close-packed metals Sc, Y, and Ru

Wolf-Dieter Schöne[1] **and Walter Ekardt**

Fritz-Haber-Institut der Max-Planck-Gesellschaft, Faradayweg 4-6, 14195 Berlin, Germany

E-mail: schoene@fhi-berlin.mpg.de

Received 5 March 2002, in final form 5 April 2002
Published 26 April 2002
Online at stacks.iop.org/JPhysCM/14/4669

Abstract

In this paper we perform a comparative study of the dynamical response of the three hexagonal close-packed metals Sc, Y, and Ru for small- and medium-sized wavevectors up to 50 eV. The calculations are based on ground states which are determined using *ab initio* pseudopotentials together with a plane-wave expansion of the wavefunctions. We consider many-body as well as crystal local-field effects which both turn out to be small. In all of the three elements we find a strong anisotropy of the response with respect to the direction of the wavevector transfer. Furthermore, we obtain almost undamped plasmon excitations for small wavevectors in the direction normal to the hexagonal planes for the response of Sc and Y.

1. Introduction

The study of electronic correlations in solids is a central topic within condensed matter physics. On the experimental side, spectroscopy has proven over time to be an extremely valuable tool in analysing electronic structure. In addition to the different types of photoemission spectroscopy and optical absorption experiments, electron energy-loss spectroscopy (EELS; see, e.g., [1]) and inelastic x-ray scattering experiments (see, e.g., [2]) have demonstrated their enormous power.

Spectroscopic experiments are especially fruitful if the experimental results can be compared to theoretical studies. In this way the various physical processes contributing to the spectra observed in the experiments can be disentangled. It has been shown that for many systems it is sufficient to consider electronic correlations within the random-phase approximation or time-dependent density-functional theory. But it also turned out that it is very important to consider the realistic band structure of the systems under consideration, i.e., to perform so-called *ab initio* calculations. The importance of this point has been shown,

[1] Author to whom any correspondence should be addressed.

0953-8984/02/184669+09$30.00

e.g., for the presumably simple nearly-free-electron (NFE) metal Al [3] and Be [4] but also for the alkali metal Cs [5] and the semiconductor Si [6].

Nowadays computers and modern *ab initio* pseudopotentials have made it possible to extend such calculations to more complicated systems. Very recently, calculations of the plasmonic excitations in Ag [7] and the response [8] and the optical absorption spectra [9] of Cu have been presented. Only this year, a joint theoretical–experimental study of the EELS spectra of rutile [10] was published.

In this article we present calculated response spectra for the hexagonal close-packed (hcp) transition metals Sc, Y, and Ru. Transition metals have a high degree of technological relevance, and understanding the electronic correlations and the interplay between electrons and the ionic lattice is important, e.g., in the context of heterogeneous catalysis.

In the following section we give a brief summary of the underlying theory, i.e., the calculation of the dynamical response and the ground-state calculations on which these calculations are based. In section 3 we present and discuss our results.

2. Theory

The differential cross section for the scattering of electrons on a many-body target can be calculated using standard first-order time-dependent perturbation theory. It is given as [11]

$$\frac{\mathrm{d}^2\sigma}{\mathrm{d}\Omega\,\mathrm{d}\omega} = \frac{m^2}{(2\pi)^3}\frac{1}{\hbar^5}v_p^2\frac{k'}{k}S(\boldsymbol{p},\omega). \tag{1}$$

Here k and k' are the absolute values of the wavevectors of the incident and the scattered particle, respectively. $\boldsymbol{p}$ is the wavevector transferred from the incident electron to the system, $\boldsymbol{p} = \boldsymbol{k} - \boldsymbol{k}'$, and $\hbar\omega$ is the transferred energy. v_p are the Fourier coefficients of the Coulomb potential, $v_p = 4\pi e^2/p^2$. Note that the wavevector $\boldsymbol{p}$ is not restricted to the first Brillouin zone (BZ).

Whereas the first part of the right-hand side of (1) contains all the information necessary for describing the particular experiment, the second part, the dynamical structure factor $S(\boldsymbol{p},\omega)$, is a ground-state property of the system under investigation. It thus represents the information about the electronic structure of the target which is to be probed by the experiment. It can be shown that $S(\boldsymbol{p},\omega)$ is proportional to the imaginary part of the generalized susceptibility or retarded density-response function (up to a factor of $\hbar$) [11]:

$$S(\boldsymbol{p},\omega) = -2\hbar V\,\mathrm{Im}\,\chi_{G=G'}(\boldsymbol{q},\omega), \tag{2}$$

where V is the volume of the system. Here we have already adopted crystal notation, using $\boldsymbol{p} = \boldsymbol{q} + \boldsymbol{G}$, with the wavevector $\boldsymbol{q}$ lying inside the BZ and $\boldsymbol{G}$ being a reciprocal-lattice vector. Equation (2) is one way of expressing the fluctuation-dissipation theorem which relates the dissipation of energy described by $\mathrm{Im}\,\chi_{G=G'}(\boldsymbol{q},\omega)$ to the electronic correlations within the system.

The task of a theory describing electron scattering experiments is therefore the calculation of the imaginary part of the retarded density-response function (in the following we suppress the word 'retarded'). Within many-body perturbation theory this can be done by solving the Bethe–Salpeter equation (BSE). In the simplest non-trivial case this leads to an expression for the density-response function within the so-called random-phase approximation (RPA). Adopting again a notation suitable for crystalline systems, $\chi_{G,G'}(\boldsymbol{q},\omega)$ is then given by the following matrix equation [12]:

$$\chi_{G,G'}(\boldsymbol{q},\omega) = \chi^{(0)}_{G,G'}(\boldsymbol{q},\omega) + \sum_{G_1,G_2}\chi^{(0)}_{G,G_1}(\boldsymbol{q},\omega)\delta_{G_1,G_2}v_{q+G_1}\chi_{G_2,G'}(\boldsymbol{q},\omega). \tag{3}$$

Here $\boldsymbol{q}$ and $\boldsymbol{k}$ denote wavevectors in the BZ, $\boldsymbol{G}$ and $\boldsymbol{G}'$ are reciprocal-lattice vectors, and j, j' are band indices. $v_{\boldsymbol{q}+\boldsymbol{G}} = 4\pi e^2/|\boldsymbol{q}+\boldsymbol{G}|^2$ is the Fourier transform of the bare Coulomb potential. $\chi^{(0)}_{\boldsymbol{G},\boldsymbol{G}'}(\boldsymbol{q},\omega)$ is the density-response function for non-interacting electrons. In a notation suitable for crystalline systems, it is given by [12–14]

$$\chi^{(0)}_{\boldsymbol{G},\boldsymbol{G}'}(\boldsymbol{q},\omega) = \frac{2}{V}\sum_{\boldsymbol{k}}^{\mathrm{BZ}}\sum_{j,j'}\frac{f_{\boldsymbol{k},j} - f_{\boldsymbol{k}+\boldsymbol{q},j'}}{\hbar\omega + \epsilon_{\boldsymbol{k},j} - \epsilon_{\boldsymbol{k}+\boldsymbol{q},j'} + \mathrm{i}\eta} \times \langle \boldsymbol{k}, j|\mathrm{e}^{-\mathrm{i}(\boldsymbol{q}+\boldsymbol{G})\cdot\hat{\boldsymbol{x}}}|\boldsymbol{k}+\boldsymbol{q}, j'\rangle\langle \boldsymbol{k}+\boldsymbol{q}, j'|\mathrm{e}^{\mathrm{i}(\boldsymbol{q}+\boldsymbol{G}')\cdot\hat{\boldsymbol{x}}}|\boldsymbol{k}, j\rangle. \tag{4}$$

Here $f_{\boldsymbol{k},j}$ denote the occupation numbers, $\epsilon_{\boldsymbol{k},j}$ the eigenvalues, and $\langle \boldsymbol{r}|\boldsymbol{k}, j\rangle = \varphi_{\boldsymbol{k},j}(\boldsymbol{r})$ the wavefunctions as obtained from a ground-state calculation within an independent-particle model. Usually this is done by solving the Kohn–Sham (KS) equations [15–17]:

$$\left(-\frac{\hbar^2}{2m}\boldsymbol{\nabla}^2 + v_{\mathrm{eff}}(\boldsymbol{r})\right)\varphi_{\boldsymbol{q},j}(\boldsymbol{r}) = \epsilon_{\boldsymbol{q},j}. \tag{5}$$

The KS equations map a system of interacting electrons onto a system of formally non-interacting (so-called KS) electrons. These electrons move in a mean-field potential which is set up by the ionic potential $v_{\mathrm{ion}}(\boldsymbol{r})$ and another term which considers the electron–electron interaction. The latter is typically split into the classical Coulomb potential of a charge distribution, $v_{\mathrm{Coul}}(\boldsymbol{r}) = \int \mathrm{d}^3r'\, n(\boldsymbol{r}')/|\boldsymbol{r}-\boldsymbol{r}'|$, and a second part, v_{xc}, in which the purely quantum-mechanical exchange–correlation contributions are considered. The effective potential is thus given as

$$v_{\mathrm{eff}}(\boldsymbol{r}) = v_{\mathrm{ion}}(\boldsymbol{r}) + v_{\mathrm{Coul}}(\boldsymbol{r}) + v_{xc}(\boldsymbol{r}). \tag{6}$$

We calculate $v_{xc}(\boldsymbol{r})$ within the local-density approximation (LDA) [16, 17] using the parametrization of the data of Ceperley and Alder [18] as obtained by Perdew and Zunger [19].

Within many-body perturbation theory it is a very tedious task to go beyond the RPA in the calculation of the density-response function. However, this can be avoided in systems in which excitonic excitations are not present. So it is perfectly sufficient in metallic systems to use the time-dependent local-density approximation (TDLDA), an extension of the LDA into the time-dependent regime. This was first done on empirical grounds by Zangwill and Soven [20] and has later been put on a solid theoretical footing by Gross and co-workers [21–23]. Within the TDLDA the density-response function is given by an extension of (3):

$$\chi_{\boldsymbol{G},\boldsymbol{G}'}(\boldsymbol{q},\omega) = \chi^{(0)}_{\boldsymbol{G},\boldsymbol{G}'}(\boldsymbol{q},\omega) + \sum_{\boldsymbol{G}_1,\boldsymbol{G}_2}\chi^{(0)}_{\boldsymbol{G},\boldsymbol{G}_1}(\boldsymbol{q},\omega)[\delta_{\boldsymbol{G}_1,\boldsymbol{G}_2}v_{\boldsymbol{G}_1}(\boldsymbol{q}) + f^{xc}(\boldsymbol{G}_1-\boldsymbol{G}_2)]\chi_{\boldsymbol{G}_2,\boldsymbol{G}'}(\boldsymbol{q},\omega). \tag{7}$$

$f^{xc}(\boldsymbol{G})$ represents vertex corrections. Within the TDLDA, f^{xc} depends only on the reciprocal-lattice vector, not on the wavevector, and is given by $f^{xc}(\boldsymbol{G}) = \int \mathrm{d}^3r\, \mathrm{e}^{-\mathrm{i}\boldsymbol{G}\cdot\boldsymbol{r}}\,[\mathrm{d}v_{xc}(\boldsymbol{r})/\mathrm{d}n(\boldsymbol{r})]$. Here $v_{xc}(\boldsymbol{r})$ is the exchange–correlation potential used in the KS equations (5). Considering vertex corrections is also referred to as taking into account many-body local-field effects. Setting $f^{xc}(\boldsymbol{G}) = 0$ recovers the RPA.

3. Results and discussion

The starting point of our calculations is a set of well-converged ground-state calculations which were done using the pseudopotential plane-wave code *fhi96md* [24] in connection with norm-conserving Troullier–Martins pseudopotentials [25, 26]. In table 1 we give some details of these calculations. In order to make sure that the pseudopotential calculations describe the ground state reliably, we also performed all-electron calculations using the full-potential

Table 1. Some characteristics of the three hcp metals considered in this paper. a_0 is the lattice constant (in Bohr) and c/a_0 the ratio of the lattice constant in the z-direction to a_0. The fourth column shows the electronic configuration of the atom used in the construction of the pseudopotential. In the fifth and sixth columns we give the number of wavevectors used to sample the BZ and the cut-off used in the expansion of the wavefunctions, respectively. The last column displays the calculated occupied bandwidth.

Element	a_0 (Bohr)	c/a_0	Atomic configuration	No of $\boldsymbol{k}$-points	Cut-off (Ryd)	Occupied bandwidth (eV)
Sc	6.255	1.594	$[Ar]3d^14s^2$	500	35	5.20
Y	6.898	1.571	$[Kr]4d^15s^2$	600	20	4.73
Ru	5.1	1.584	$[Kr]4d^75s^1$	500	40	8.36

linearized augmented-plane-wave (FPLAPW) code WIEN95 [27]. The results obtained with these two approaches agree perfectly for the valence bands and the low-lying conduction bands. As usual, there are differences for the high-lying conduction bands which we attribute to errors due to the linearization done in the LAPW formalism [28].

The pseudopotential calculations of the ground state, on which the following determination of the dynamical response is based, have been done considering only the nd and $(n+1)$s electrons as valence electrons, where $n = 3, 4$. The corresponding ns and np electrons have been assigned to the core and are considered via the pseudopotential. In other words, we do not consider explicitly the semicore states. This approach is perfectly sufficient as long as ground-state properties are considered and it is also sufficient for the calculation of the low- and intermediate-energy region of the dynamical response [7, 8].

Having obtained a reliable ground state, the major task is the calculation of the independent-particle density-response function from (4). In the calculation of $\chi^{(0)}_{\boldsymbol{G},\boldsymbol{G}'}(\boldsymbol{q},\omega)$ we used 100 bands in order to ensure convergence of the sum with respect to the number of bands in the energy region considered. For η we chose 0.2 eV, which is small enough for us to avoid an artificial broadening of the resulting spectra but large enough for us to obtain stable results using a reasonable sampling of the BZ. In the cases of Sc and Y the BZ was sampled by a $10 \times 10 \times 5$ mesh; in the case of Ru we used $10 \times 10 \times 6$ wavevectors for the sampling.

For each of the three elements under consideration we calculated the dynamical response for four small- and medium-sized wavevectors. For each wavevector the response was determined within the RPA and the TDLDA. For all elements we found that including the vertex corrections as considered within the TDLDA leads only to minor changes in the results. Although this is a different behaviour to that found for simple metals like Al [3], in which including these vertex corrections leads to small but important changes in the spectra, our results are in accordance with results obtained recently for rutile [10]. Furthermore, we considered up to four shells of reciprocal wavevectors in equations (3) and (7), i.e., we took crystal local-field effects into account. In table 2 we give an overview over the shell structure of the reciprocal-lattice vectors of hcp lattices for the first four shells.

In figure 1 we summarize our results for the imaginary part of the density-response function of Sc for the four wavevectors $\boldsymbol{q} = (0, 0, 0.2)$, $\boldsymbol{q} = (0, 0, 0.4)$, $\boldsymbol{q} = (0.1, 0.1, 0)$, and $\boldsymbol{q} = (0.3, 0.3, 0)$, given in units of $2\pi/a_i$ (see the caption of table 2). All results displayed were obtained within the TDLDA and considering four shells of reciprocal-lattice vectors. As already mentioned, for Sc the inclusion of many-body or crystal local-field effects does not lead to significant changes of Im $\chi_{\boldsymbol{G},\boldsymbol{G}'}(\boldsymbol{q},\omega)$.

Comparing the two plots on the left-hand side of figure 1 with those on the right-hand side shows a remarkable qualitative difference. For a small wavevector transfers $\boldsymbol{q}$ along the

Table 2. The shell structure of the reciprocal-lattice vectors $\boldsymbol{G}$ for hcp lattices. The $\boldsymbol{G}$ are given in cartesian coordinates in units of $2\pi/a_i$, with $a_1 = \sqrt{3}\,a_0$, $a_2 = a_0$, and $a_3 = c$. As usual, c is the lattice constant in the z-direction.

Shell	G_x	G_y	G_z	Number	Total
Scalar	0	0	0	1	1
1	0	0	±1	2	3
2	±1	±1	0	4	
	±2	0	0	2	9
3	0	0	±2	2	11
4	±1	±1	±1	8	
	±2	0	±1	4	24

z-direction, Im $\chi_{G,G'}(\boldsymbol{q}, \omega)$ displays only a single, though broad peak around 13 eV with some additional structure at lower energies. For comparison we also calculated the response within the jellium model for a Wigner–Seitz radius of $r_s = 2.38$ which corresponds to the average electronic density of the valence electrons of Sc, $n = 0.0178$ Bohr^{-3}, and used a wavevector of the same length. The peak position of the jellium response is almost at the same position as the one obtained for Sc. However, the widths of the two structures are drastically different. Whereas the width of the jellium response is solely due to the numerical value of $\eta = 0.2$ eV, the width of the Sc response is much wider, a result of one-electron interband transitions which are not possible in the homogeneous electron gas. We checked this by calculating the response using values for η of 0.1, 0.2, and 0.4 eV. In each case the width of the peak was the same. Note that the Fermi energy for a homogeneous electron gas with $r_s = 2.38$ is much larger (8.85 eV) than the Fermi energy for Sc. However, the Wigner–Seitz radius which corresponds to $E_F = 5.2$ eV is 3.10, being much larger than 2.38. The corresponding plasma frequency would therefore be at much lower energies. One has to keep in mind, however, that when comparing *ab initio* results with results obtained within the jellium model one always has the problem of deciding which parameter should be fixed, the average electronic density, the Fermi energy, etc. For non-NFE metals in particular, each choice leads to different results.

We also calculated the response for a larger wavevector transfer in the z-direction. In this case the peak becomes even wider and there is more structure at lower energies. Also the agreement with the corresponding jellium calculation is less good than in the first case. But, nevertheless, the basic structure of Im $\chi_{G,G'}(\boldsymbol{q}, \omega)$ in this case is still a rather well-defined peak.

The situation changes drastically if the response is calculated for wavevectors within the hexagonal plane ($z = 0$). The plot in the upper right of figure 1 shows Im $\chi_{G,G'}(\boldsymbol{q}, \omega)$ for a wavevector whose magnitude is even slightly smaller than the one considered for the plot shown in the upper left part of figure 1. The imaginary part of the response function for $\boldsymbol{q} = (0.1, 0.1, 0)$ shows two distinct peaks around 20 eV within an otherwise broad structureless behaviour known from systems with d bands [7, 8]. This applies also to the last plot shown in figure 1 for $\boldsymbol{q} = (0.3, 0.3, 0)$ although here the structure between 10 and 20 eV is more pronounced. This means that for these wavevectors the calculated spectra of Sc show a behaviour which is typical for transition metals, contrary to the jellium-like structure of Im $\chi_{G,G'}(\boldsymbol{q}, \omega)$ for wavevectors in the z-direction.

The plots displayed in figure 1 raise two questions. First, are the excitations which occur for wavevector transfers perpendicular to the hexagonal planes really plasmon excitations as suggested by the comparison with the jellium results? And second, has Sc, in this direction, really got jellium-like properties?

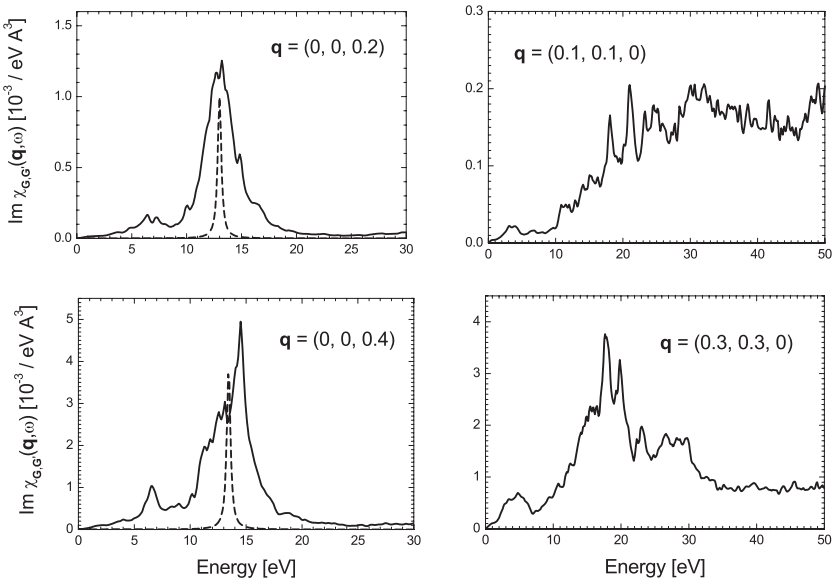

Figure 1. The imaginary part of the density-response function for Sc (solid curves) calculated for four small- and medium-sized wavevectors. All calculations were done using TDLDA and including four shells of $\boldsymbol{G}$-vectors. Here, as throughout the text, wavevectors are given in units of $2\pi/a_i$ (see the caption of table 2). In all cases $\boldsymbol{G} = \boldsymbol{G}' = 0$. The dashed curves denote the result of a jellium calculation using $r_s = 2.38$ which corresponds to the average electronic density of Sc. Note that in this plot and in figure 3 the unit of the jellium result is 10^{-2} eV^{-1} Å^{-3}.

The first question is most easily answered by inspection of the dielectric function, $\epsilon_{G=G'=0}(\boldsymbol{q}, \omega)$, for $\boldsymbol{G} = \boldsymbol{G}' = 0$ as displayed in the top left corner of figure 2 for the wavevector $\boldsymbol{q} = (0, 0, 0.2)$. The plot shows clearly that the real part (solid curve) has a zero around 13 eV, exactly at the energetic position at which the excitation occurs. A more detailed view of the region of interest is given in the inset. For these energies the imaginary part of $\epsilon_{G=G'=0}(\boldsymbol{q}, \omega)$—which is proportional to the imaginary part of $\chi^{(0)}_{G,G'}(\boldsymbol{q}, \omega)$—has almost dropped to zero. This indicates that the peaks in the response of Sc for wavevectors in the z-direction are indeed due to plasmon excitations.

An answer to the second question is provided by a plot of the imaginary part of the density-response function for non-interacting particles, $\chi^{(0)}_{G,G'}(\boldsymbol{q}, \omega)$, as shown by the solid curve in the lower left plot of figure 2. The deviation of this curve and the corresponding curve for the homogeneous electron gas for the same wavevector (dashed curve) is obvious and this clearly shows that Sc is definitely not a jellium-like metal. The plasmon in Sc originates from more general grounds; because the imaginary and real parts of the density-response function are related by the Kramers–Kronig relation the fast decay of Im $\chi^{(0)}_{G,G'}(\boldsymbol{q}, \omega)$ leads to the fact that the real part has reached its asymptotic region—in which it decays as ω^{-2}—already at around 10 eV, lying on top of the jellium result. This is shown in the inset of the lower left plot of figure 2.

For wave transfers parallel to the hexagonal plane the situation is completely different. The solid curve in the lower right plot of figure 2 denotes Im $\chi^{(0)}_{G,G'}(\boldsymbol{q}, \omega)$ for $\boldsymbol{q} = (0.1, 0.1, 0)$. One clearly notices a slower decay which is interrupted by additional peaks which represent transitions to higher-lying bands. The peak structure between 5 and 10 eV, e.g., is caused by transitions from the valence bands to the three bands marked by the thick solid curves in

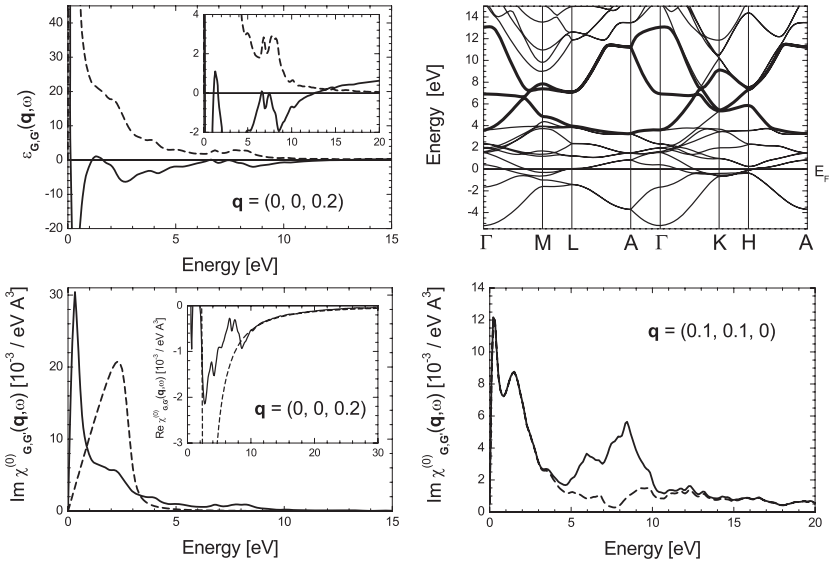

Figure 2. Plots to illuminate the behaviour of Sc as shown in figure 1. The plot in the upper left corner shows the real (solid curve) and imaginary (dashed curve) parts of the dielectric function. The plot below displays the imaginary part of the density-response function for Sc (solid curve) and the homogeneous electron gas (dashed curve). In the inset the real part is shown. In order to avoid misunderstandings, we stress that here the results for Sc and the homogeneous electron gas are in the same units. The plot in the upper right corner is the band structure of Sc and the one in the lower right corner is again Im $\chi_{G,G'}(\boldsymbol{q},\omega)$. In all plots $\boldsymbol{G} = \boldsymbol{G}' = 0$. For further explanations see the main text.

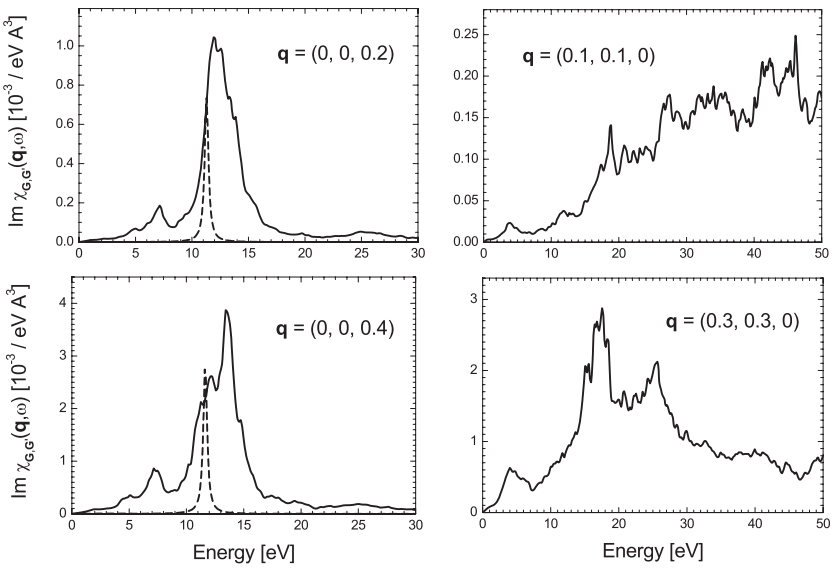

Figure 3. As figure 1, but for Y. Up to details, the displayed density-response functions for Y resemble very much these of Sc. The Wigner–Seitz radius used for Y is $r_s = 2.61$.

the band structure of Sc shown in the upper right plot of figure 2. This can be visualized by excluding these bands in the summation of (4) which leads to the dashed curve. From this

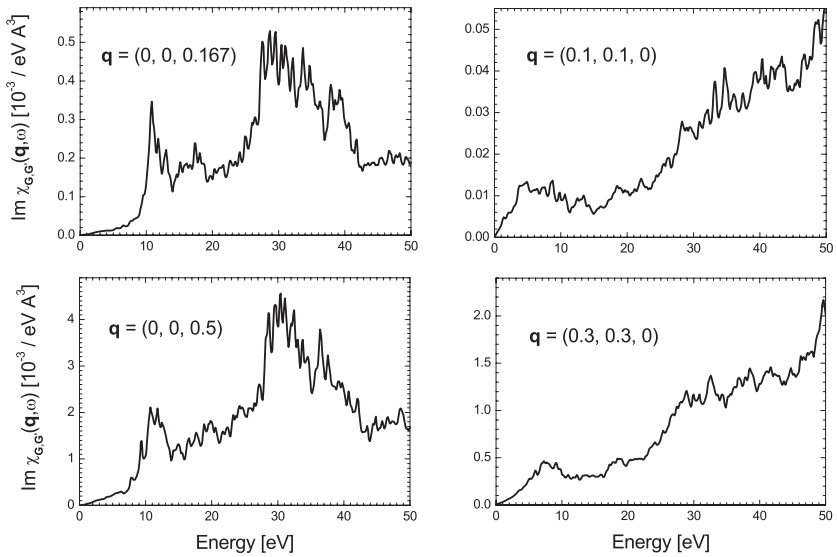

Figure 4. As figure 1, but for Ru. Whereas the spectra for $\boldsymbol{q} = (0, 0, z)$ are markedly different from those for Sc and Y, the response for wavevectors which are within the hexagonal planes is similar.

we conclude that transitions to higher excited bands are completely missing in the density-response function for independent particles for wavevectors perpendicular to the z-direction. This in turn leads to the plasmon excitations observed in the left panel of figure 1.

Figure 3 shows the calculated density-response functions for Y for four wavevectors with the same relative coordinates as in the case of Sc. The plots are very similar to the ones of Sc. Again, Im $\chi_{G,G'}(\boldsymbol{q}, \omega)$ for wavevectors in the z-direction reveals a clear plasmon excitation, although the peak positions of the density-response functions of Y are more shifted towards higher energies with respect to the corresponding jellium curves than was the case for Sc.

In figure 4 we show density-response functions for four different wavevectors for Ru. Again there is a manifest difference between the results for wavevectors in the z-direction and those perpendicular to this direction. However, the Im $\chi_{G,G'}(\boldsymbol{q}, \omega)$ plotted for $\boldsymbol{q} = (0, 0, 0.167)$ and $\boldsymbol{q} = (0, 0, 0.5)$ display much more structure than just a single peak. In both curves there is a distinct local maximum around 11 eV. This peak coincides with a zero of the real part of the dielectric function, i.e., the peak resembles a plasmon excitation which is damped by single-particle transitions, represented by a non-vanishing imaginary part of $\epsilon_{G=G'=0}(\boldsymbol{q}, \omega)$. In addition, there is a structure of several peaks around 30 eV. The curves for $\boldsymbol{q} = (0.1, 0.1, 0)$ and $\boldsymbol{q} = (0.3, 0.3, 0)$ show an overall shape which is similar to the ones for Sc and Y.

4. Conclusions

We have calculated the density-response function for the three hcp metals Sc, Y, and Ru for small- and medium-sized wavevectors. For all three elements we find a strong anisotropy for wavevector transfers parallel to the z-direction and wavevectors within the hexagonal plane. Even more amazing are the results for Sc and Y, where the imaginary parts of the density-response functions for wavevectors in the z-direction clearly reveal plasmon excitations. For directions parallel to the hexagonal plane the density-response function for all three elements resembles the structure known from noble metals. In all three metals many-body and crystal local-field effects can almost be neglected.

Acknowledgments

G Ertl is gratefully acknowledged for his interest and generous support. We thank M Bacelar and R Keyling for enlightening discussions. This work was supported by the Deutsche Forschungsgemeinschaft through SFB 450.

References

[1] vom Felde A, Sprösser-Prou J and Fink J 1989 *Phys. Rev.* B **40** 10 181
[2] Schülke W 1991 *Handbook of Synchrotron Radiation* vol 3, ed G Brown and D E Moncton (Amsterdam: Elsevier)
[3] Fleszar A, Quong A A and Eguiluz A G 1995 *Phys. Rev. Lett.* **74** 590
[4] Maddocks N E, Godby R W and Needs R J 1994 *Phys. Rev.* B **49** 8502
[5] Fleszar A, Stumpf R and Eguiluz A G 1997 *Phys. Rev.* B **55** 2068
[6] Walter J P and Cohen M L 1972 *Phys. Rev.* B **5** 3105
[7] Cazalilla M A, Dolado J S, Rubio A and Echenique P M 2000 *Phys. Rev.* B **61** 8033
[8] Campillo I, Rubio A and Pitarke J M 1999 *Phys. Rev.* B **59** 12 188
[9] Marini A, Onida G and Sole R D 2001 *Phys. Rev.* B **64** 195125
[10] Vast N, Reining L, Olevano V, Schattschneider P and Jouffrey B 2002 *Phys. Rev. Lett.* **88** 037601
[11] Nozières P 1997 *Theory of Interacting Fermi Systems* (Reading, MA: Addison-Wesley)
[12] Eguiluz A G, Fleszar A and Gaspar J A 1995 *Nucl. Instrum. Methods Phys. Res.* B **96** 550
[13] Adler S L 1962 *Phys. Rev.* **126** 413
[14] Wiser N 1963 *Phys. Rev.* **129** 62
[15] Hohenberg P and Kohn W 1964 *Phys. Rev.* **136** B864
[16] Kohn W and Sham L J 1965 *Phys. Rev.* **140** A1133
[17] Dreizler R M and Gross E K U 1990 *Density Functional Theory* (Berlin: Springer)
[18] Ceperley D M and Alder B J 1980 *Phys. Rev. Lett.* **45** 566
[19] Perdew J P and Zunger A 1981 *Phys. Rev.* B **23** 5048
[20] Zangwill A and Soven P 1980 *Phys. Rev.* A **21** 1561
[21] Gross E K U and Kohn W 1985 *Phys. Rev. Lett.* **55** 2850
Gross E K U and Kohn W 1986 *Phys. Rev. Lett.* **57** 923 (erratum)
[22] Petersilka M, Grossmann U J and Gross E K U 1996 *Phys. Rev. Lett.* **76** 1212
[23] Gross E K U, Dobson J F and Petersilka M 1996 *Density Functional Theory (Springer Topics in Current Chemistry vol 181)* ed R F Nalewajski (Berlin: Springer) p 81
[24] Bockstedte M, Kley A, Neugebauer J and Scheffler M 1997 *Comput. Phys. Commun.* **107** 187
[25] Troullier N and Martins J L 1991 *Phys. Rev.* B **43** 1993
[26] Fuchs M and Scheffler M 1999 *Comput. Phys. Commun.* **119** 67
[27] Blaha P, Schwarz K, Dufek P and Augustyn R 1995 *WIEN95* Technical University of Vienna
This is an improved and updated Unix version of the original copyrighted WIEN code, which was published by Blaha P, Schwarz K, Sorantin P and Trickey S B 1990 *Comput. Phys. Commun.* **59** 399
[28] Schöne W-D, Keyling R, Bandić M and Ekardt W 1999 *Phys. Rev.* B **60** 8616